

THE RF SYSTEM OF THE SUPERCONDUCTING CYCLOTRON AGOR\*

S. Brandenburg, C. Bieth, G. Coeur-Joly, J.P. Chauvin, R. Eyraud,  
V. Hervier, J. Lebris and B. Monsanglant

AGOR project

Institut de Physique Nucléaire, 91406 Orsay Cedex, France and  
Kernfysisch Versneller Instituut, 9747 AA Groningen, the Netherlands

**ABSTRACT**

The RF system of the superconducting cyclotron AGOR is described. The design of the resonators is discussed. The calculated resonator properties are compared with the model measurements. The RF power amplifiers and the regulation system are shortly discussed.

**INTRODUCTION**

The superconducting cyclotron AGOR is presently being constructed by a French-Dutch collaboration at Orsay, France. After beam tests in Orsay the cyclotron will be installed in Groningen, the Netherlands, in 1992. It will accelerate light and heavy ions for research in nuclear physics. The energy ranges from 200 MeV for protons to 6 MeV per nucleon for heavy ions with  $Q/A \leq 0.20$ .

The characteristics of the cyclotron are summarized in ref. 1; a detailed description is given in ref. 2 while the present status of the project is discussed in ref. 3.

**RESONATOR DESIGN**

The symmetry with respect to the median plane of the accelerating field required in a superconducting cyclotron with axial injection implies the use of a symmetric resonator. Taking into account the geometrical constraints a  $\lambda/2$  resonator with a spiralled electrode in the median plane is the only realistic solution<sup>4</sup>.

The energy range given above and the threefold symmetry of the cyclotron require a frequency range 24 - 62 MHz for the resonators and the use of harmonic modes  $h = 2; 3$  and 4. The relatively high frequency to be obtained excludes the use of a vacuum feedthrough between the electrode and the coaxial line. This has important consequences for the design of the resonators, both from a mechanical and an RF point of view.

The absence of a feedthrough implies that the electrode is held via the inner conductor of the coaxial line, which has a length of several meters. Taking into account the position tolerances (0.3 mm in the central region, 0.5 mm at extraction radius) it is necessary to minimize the length of the coaxial line, i.e. maximize its characteristic impedance.

The value of the characteristic impedance is constrained by the maximum diameter of the hole that can be made in the yoke inbetween two flutter poles and by the minimum diameter of the inner conductor of the coaxial line. The latter is determined by the rigidity required and by the maximum acceptable current density in the contacts between the sliding short and the inner conductor.

A further shortening of the length of the coaxial line may be obtained by carefully shaping the transition between the electrode and liner and the coaxial line: a decrease of the characteristic impedance of the transition will shorten the coaxial line at low frequencies, while at the same time lengthening it at high frequencies. Although this lengthening is accompanied by an increase of the current in the shorting plate, it presents an interest because its distribution becomes more homogeneous.

The position on the electrode of the connection to the inner conductor of the coaxial line has a strong effect on the radial voltage distribution and thus on the power dissipation. The effective position of the connection between electrode and inner conductor has been displaced outwards with respect to the axis of the inner conductor to minimize the power dissipation, while maintaining a voltage distribution that increases slightly with radius.

**Tuning and Coupling**

The feedback system for maintaining the tuning is acting on the position of the shorting plate. In order to obtain a sufficient sensitivity the shorting plate consists of two concentric rings, the main and intermediate short, which can move with respect to each other (fig. 1).

The feedback and fine tuning act on the relative distance between the main and intermediate short, while the coarse initial tuning is obtained by displacing the two shorts together. The sensitivity is maximized by using the relative distance between the two shorts on one side of the resonator only.

The resonators are coupled to the RF amplifiers via a coaxial line of about 20 m and an inductive

coupling loop mounted on one of the shorting plates. The area of the loop has to be variable in order to match the impedance of the resonator to the characteristic impedance of the feeder. The variable loop area is obtained by varying the distance between the main and intermediate short as a function of frequency. Interference between the different regulation systems is avoided by not using the shorting plate carrying the coupling loop for the feedback system.

Although the inductive coupling complicates the construction of the shorting plate and its displacement mechanism we prefer it over capacitive coupling for a number of reasons. Inductive coupling does only weakly excite higher order modes across the electrodes. Since the single turn extraction aimed at sets severe limits on the excitation of such modes, this is an important advantage. A discharge in the resonator causes very high voltages in the vacuum feedthrough of the feeder with the consequent risk of breakdown for capacitive coupling, while for inductive coupling the feeder is terminated by a very low impedance. Finally the constraints on the resonator discussed above do not leave enough space to implement a capacitive coupling.

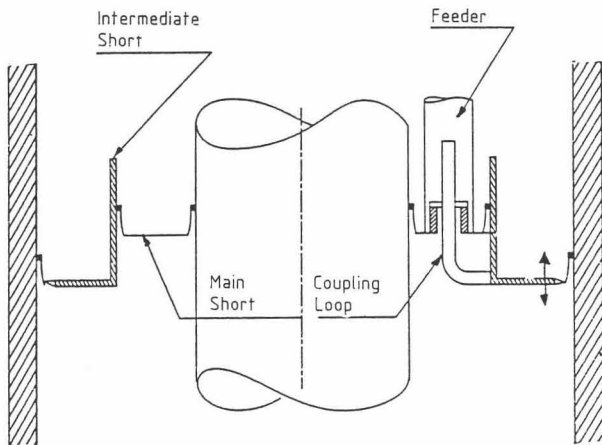


fig. 1 Schematic drawing of the shorting plate and coupling loop

**Calculations**

The properties of the resonator were calculated by assuming it to be a sequence of series and parallel transmission lines. For the coaxial lines the characteristic impedances were obtained analytically, for the electrode the method of curvilinear squares was used, with estimated equipotentials on the electrode as a starting point.

The result of the method of curvilinear squares was verified for a few cases by tracing the equipotentials between electrode and liner on resistive paper or by measuring directly the resistance of the cross section on the resistive paper. The different methods were found to agree within  $\leq 5\%$ .

The characteristic impedances and lengths of all transmission lines being known the position of the shorting plate and the voltage distribution along the accelerating gaps are easily

calculated as a function of frequency. Taking into account the discontinuity due to the intermediate shorting plate leads to an increase of the length of the coaxial line of at most 10 mm.

The power dissipation was determined by distributing the currents according to the estimated current lines and calculating the corresponding power distribution. In calculating the power dissipation the measured RF resistance of the sliding contacts on the shorting plate was used.

In fig. 2 the required RF power and the current density in the sliding contacts are shown as a function of frequency. The Q-value of the resonators varies between 6500 and 7300 over the full frequency range. The maximum density under operational conditions is 3650 A/m and the maximum power 34 kW, both at a frequency of 62 MHz, where a voltage of 76 kV at injection radius is required. The error of the calculations is estimated to be  $\leq 20\%$  for the power and Q-factor,  $\leq 10\%$  for the current and  $\leq 20\text{ mm}$  for the position of the shorting plate.

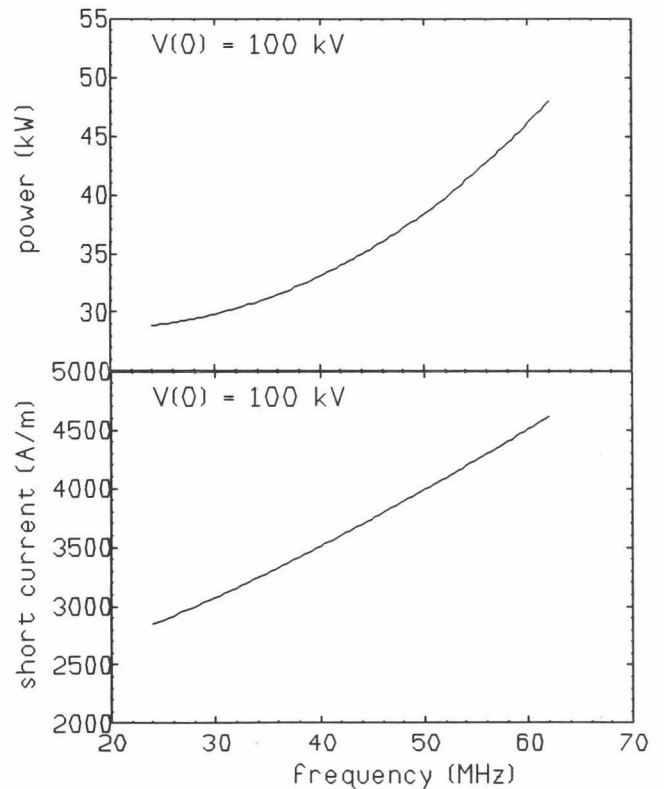


fig. 2 Calculated power dissipation and current density in the shorting plate for 100 kV at injection radius

**Model Measurements**

In order to verify the calculations a full scale model with a reduced frequency range (46 - 62 MHz) was constructed. The coaxial lines were made of copper, while the electrode and liner were made of plywood covered with a self-adhesive copper tape of 35  $\mu\text{m}$  thickness.

The measured voltage distribution for the two accelerating gaps is shown in fig. 3 together

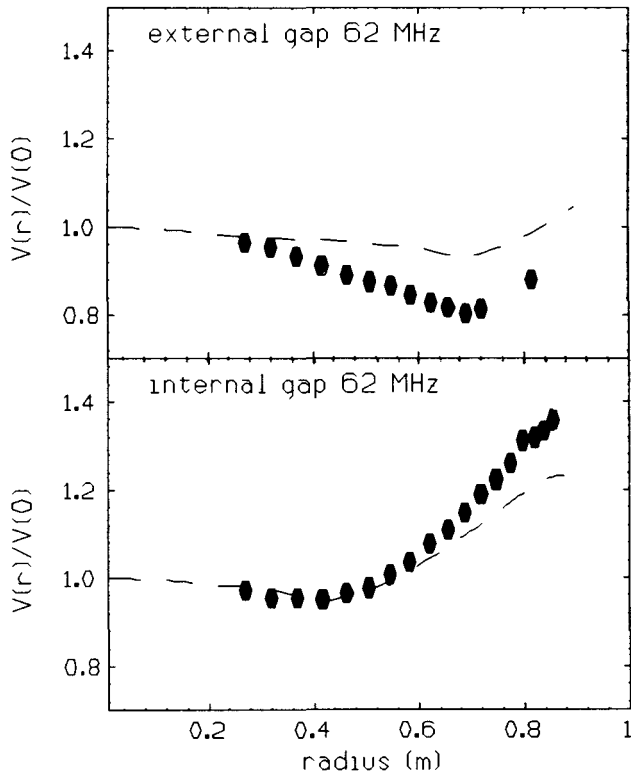


fig. 3 Measured (full circles) and calculated (dashed lines) voltage distributions along the acceleration gaps

with the result of the calculations made before the measurements. The measured distributions were used to correct the equipotentials on the electrode defining the cross sections of the transmission lines. The calculation with the corrected characteristic impedances and lengths of the transmission lines fits the measured voltage distributions.

The measured position of the shorting plate is shown in fig. 4 together with the result of two calculations. The dashed line represents the calculation made before the measurements, the full line the calculation taking into account the measured voltage distributions.

The inhomogeneity of the current distribution in the sliding contacts was measured with 12 loops mounted on the shorting plate. It was found to be less than 15 %.

The model has also been used to study the frequency of the  $3\lambda/2$  mode as a function of the frequency of the  $\lambda/2$  mode. The ratio was found to close to 3 but by dissymetrizing the short positions the excitation of the  $3\lambda/2$  mode by the third harmonic in the driving signal can be suppressed.

Transverse modes across the electrode were found at 113 and 137 MHz and their harmonics. The signal from a pickup loop in the shorting plate at these frequencies is very small, indicating that these modes are indeed very weakly coupled to the coupling loop.

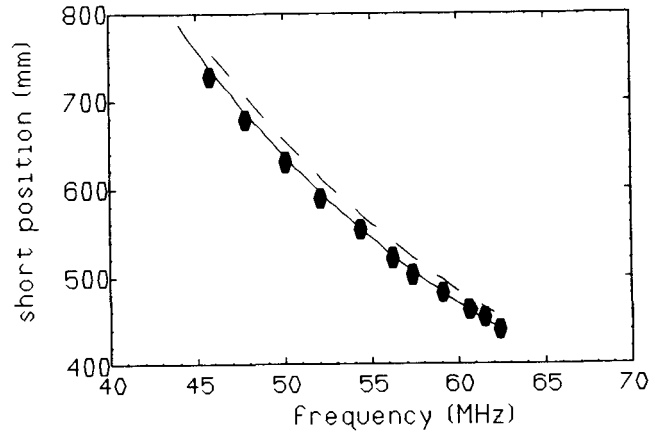


fig. 4 Measured (full circles) and calculated (full and dashed lines) positions of the shorting plate.

#### Sliding Contacts

As was discussed above the sliding contacts between the shorting plate and the coaxial line are located in vacuum, while they should also allow the shorting plate to move under power. The study of the electrical and mechanical properties of the contacts has allowed the optimization of the various parameters of the contact as a function of constraints such as current density and mechanical tolerance.

A special resonator has been built to test the contacts at 27 and 60 MHz at the required current density. The measured and calculated temperature of the contacts<sup>6)</sup> are shown in fig. 5. The contacts that will be used in the resonators allow a maximum current density of 5500 A/m for a mechanical tolerance of 0.3 mm.

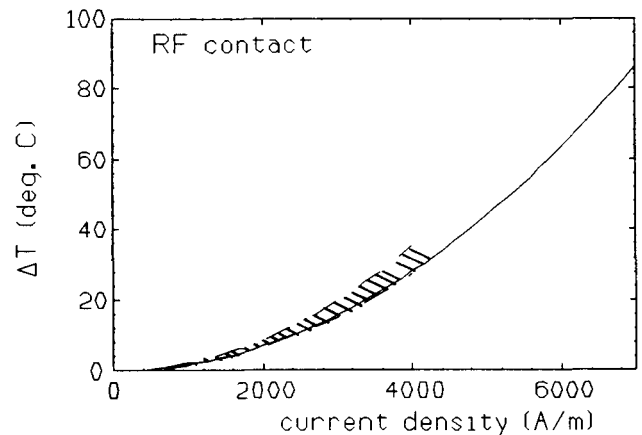


fig. 5 Calculated (full line) and measured (hatched area) temperatures of the sliding contacts as a function of current density at 60 MHz.

### Present Status

The RF design and the measurements on the scale model have been completed. The engineering design has started in April 1988 and is almost completed. A call for bids for the construction of the resonators has been sent out at the end of April. The construction of the resonators is expected to start in September 1989 and the three resonators should be completely installed by September 1991.

### POWER AMPLIFIERS

The RF power needed for the resonators is furnished by three 70 kW tuneable amplifiers. The amplifiers require 0.6 W input power and consist of a 2 kW solid state broadband amplifier and a tuned endstage with a Siemens RS2058 tetrode in a grounded cathode configuration.

In order to obtain the required phase and gain stability a regulation system will be installed in the amplifiers.

The factory acceptance tests of the first amplifier will take place in May 1989, delivery and acceptance tests at the AGOR site are planned for June 1989. The remaining two amplifiers will be delivered in September 1989.

### REGULATION SYSTEMS

The electronic regulation systems for the resonators have to be rather performing in order to allow the single turn extraction of light ion beams aimed at:

- voltage stability	$10^{-4}$
- voltage accuracy	$10^{-3}$
- phase stability & accuracy	$0.1^\circ$

The use of harmonic modes  $h = 2; 3$  and  $4$  requires a relative phase between the resonators of either  $0^\circ$  or  $\pm 120^\circ$ . These relative phases are obtained by mixing a variable frequency signal (424 - 462 MHz) with three signals of 400 MHz with the proper phases. The 400 MHz signals are generated with a VCO, using a fixed 10 MHz signal of the synthesizer as a reference.

For the phase and amplitude detectors it was found necessary to mount them in a temperature stabilized box to obtain the required stability. The temperature stabilization made it possible to simplify the amplitude detector considerably: a compensating bridge with selected diodes turned out to be unnecessary.

The phase detector performs a direct phase measurement without an intermediate frequency and uses fast ECL flipflops<sup>6)</sup>. The main problem is posed by the walk due to the variation of the amplitude of the signal from the resonator, which amounts to 15 dB. By a careful design of the lay-out of the components and by using selected components it has been possible to limit the walk to  $1^\circ$ .

For the amplitude and phase modulator care has been taken to increase their bandwidth as much as possible in order to simplify the overall transfer function of the system, which will be determined by the resonator. It has been possible to obtain a bandwidth of  $\approx 100$  kHz for both, to be compared with a bandwidth  $\leq 12$  kHz for the resonator.

### Present Status

The design and testing of the RF modules of the regulation system has been completed; the series production of the modules will be finished by the end of 1989. The design of the correcting and amplifying circuits will be completed in the next few months and series production should be finished by the end of the year. A complete system will be available in September 1989 and will be tested with the 60 MHz test resonator and the 70 kW power amplifier.

\* Work jointly supported by the Institut National de Physique Nucléaire et de Physique des Particules (IN2P3), France and the Stichting voor Fundamenteel Onderzoek der Materie (FOM), the Netherlands.

### REFERENCES

- 1) S. Galès, AGOR: a superconducting cyclotron for light and heavy ions, Proc. 11th Conf. on Cyclotrons and their Applications, Tokyo, 1986, pg. 184-190
- 2) AGOR design report (unpublished), 1986
- 3) H.W. Schreuder, The AGOR cyclotron past the half way mark, Proc. 12th Conf. on Cyclotrons and their Applications, Berlin 1989
- 4) C. Bieth, Le système accélérateur HF du projet AGOR, AGOR internal report, 1985
- 5) B. Monsanglant et al., Résultats des essais de contact type MK1 à 60 MHz, AGOR internal report 1986
- 6) J. Lebris, Discriminateur de phase, AGOR internal report 1988